7. Knutsson, A., Hammar, N. and Karlsson, B., *Chronobiol. Int.*, 2004, **21**, 1049–1053.
8. Åkerstedt, T., Kecklund, G. and Johansson, S.-E., *Chronobiol. Int.*, 2004, **21**, 1055–1061.
9. Taylor, P. J. and Pocock, S. J., *Br. J. Ind. Med.*, 1972, **29**, 201–207.
10. Bøggild, H., Suadicani, P., Hein, H. O. and Gyntelberg, F., *Occup. Environ. Med.*, 1999, **56**, 640–645.

ACKNOWLEDGEMENTS. We thank Arti Parganiha for discussions and suggestions. The University Grants Commission, New Delhi supported this work through DRS-SAP sanctioned to the School of Life Sciences, Pt. Ravishankar Shukla University, Raipur in the thrust area of research in chronobiology. We are grateful to the Dy. FA & CAO (G), South-Eastern Central Railway, Bilaspur for providing us access to their employees' database.

Received 20 March 2006; revised accepted 5 October 2006

ATANU KUMAR PATI*
K. VENU ACHARI

School of Life Sciences,
Pt. Ravishankar Shukla University,
Raipur 492 010, India
**For correspondence.*
e-mail: akpati19@hotmail.com

Quantification of trace gas emissions from shifting cultivation areas using remote sensing and ground-based measurements

Shifting cultivation, also known as slash-and-burn cultivation, is widespread in the northeastern region of India and causes ecological loss to the forests and environment. It is locally called as 'jhum' and is practised by indigenous tribes during dry months of February to March every year. In India, 55% of the total forest cover is prone to fires annually[1] and major contribution comes from shifting cultivation. Recurrent forest fires result in loss of forest cover, erosion of topsoil, desertification and decline in forest productivity[2]. Studies reveal that tropical biomass burning is a significant source of organic carbon to the atmosphere[3,4], producing large amounts of trace gases and aerosol particles, which play a pivotal role in tropospheric chemistry and climate[5]. Aerosols containing black carbon are emitted primarily in the tropical and subtropical regions of the world[6], accounting for the release of almost 100 million tons of smoke aerosols into the atmosphere as a result of biomass burning[7]. These submicron smoke aerosols play a major role in radiation balance of the earth–atmospheric system[8], by reflecting a portion of the incoming solar radiation back to space, thereby reducing the amount of sunlight reaching the earth's surface[9,10]. In addition, aerosols from burning serve as cloud-condensation nuclei and alter the properties of the boundary-layer clouds[11]. Due to forest fires, there is widespread concern about the loss of biodiversity, spread of human and plant diseases through colonization, increase in concentration of greenhouse gases, changes on the earth's radiative energy budget, effects on atmospheric chemistry and increase in surface albedo and water run-off.

Biomass burning releases trace gases such as carbon dioxide, methane, nitrous oxide and particles (smoke carbon). In addition, biomass burning perturbs the other components of the earth system, including biogeochemical cycling of nitrogen and carbon (CO_2, CO and CH_4); water run-off and evaporation affecting the hydrological cycle; reflectivity and emissivity of land, which in turn alters the radiative properties of land, and stability of the ecosystems, which in turn impacts biological diversity[12]. Vegetation burning has also been shown to play an important role in annual fluxes of many trace gases to the troposphere and enough evidence exists to show that biomass burning is an important driver of global change[13–15].

Considering the above impacts, information on the location, size, timing of fire, maps of the areas burnt, characterization of fuel and combustion conditions along with the amount of greenhouse gases emitted is required to understand the impact of biomass burning on the atmospheric environment[12,16]. Remote sensing technology, with its multi-temporal, multi-spectral, repetitive and synoptic coverage, provides valuable information on various fire events in a timely and cost-effective manner. Although the potential of remote sensing technology for biomass burning and fire detection studies is widely recognized, the present regional and global active fire products are widely underutilized by fire managers and their quality needs considerable enhancement, to meet the needs of local user communities[17]. For fire monitoring and burnt area estimation, the general consensus from recent studies is that, data provided by coarse resolution satellites such as NOAA AVHRR at 1 km sensor were of limited use[18]. It was considered to be in general unsuitable to provide reliable estimates of fire activity, especially considering its geographical extent. In case of satellite data with low spatial resolution, fires cannot be accurately assigned to forest or agriculture. Under these circumstances, the data are unreliable for emission estimates. Further, sensitivity to the proportion of pixels that are burnt, i.e. the size and spatial distribution of the burnt areas relative to the sensor spatial resolution, was similarly considered to be a significant factor. Considering these issues due to low spatial resolution of coarse-resolution satellite datasets, evaluation of different sensors with relatively high-to-moderate resolution for burnt-area detection at local scale was considered an area of potential research. In the present study, Indian Remote Sensing Satellite (IRS-P6) – Advanced Wide Field Sensor (AWiFS) temporal data from January to April 2005 covering the northeastern region were used for quantifying greenhouse gas emissions.

Northeast India comprises seven sister states, viz. Assam, Arunachal Pradesh, Manipur, Meghalaya, Mizoram, Nagaland and Tripura. They are bordered by Bhutan and China in the north, Myanmar in the south and southeast, and Bangladesh in the west. Perennial rivers like the Brahmaputra flow through this region. The Brahmaputra valley is a meeting ground of the temperate east Himalayan flora and the wet evergreen and wet deciduous flora. Major forest types found in the study area are tropical evergreen and semi-evergreen, moist deciduous forest, bamboo brakes, Dipterocarpus, grasslands, riverain, sal, teak, pine, etc.[19]. The tropical vegeta-

Table 1. State-wise statistics of total emissions

Total emissions (Tg)	Arunachal Pradesh	Assam	Manipur	Meghalaya	Mizoram	Nagaland	Tripura	Sum
CO_2	0.0002649	1.169E-06	5.147E-05	0.0009006	0.0010929	0.0008903	0.0003274	0.0035286
CO	1.5864E-05	8.4528E-08	2.1324E-06	5.3233E-05	6.6743E-05	4.6442E-05	1.9265E-05	0.00020376
CH_4	1.0865E-06	5.8995E-09	1.7175E-07	4.0838E-06	3.8986E-06	2.7898E-06	1.1327E-06	1.3169E-05
NO	3.36973E-07	1.52032E-09	9.94663E-08	1.67721E-06	2.0802E-06	1.42512E-06	3.16701E-07	5.9372E-06
N_2O	3.48403E-08	1.41874E-10	7.56107E-09	1.19744E-07	1.57444E-07	1.31083E-07	4.43286E-08	4.95143E-07
$PM_{(2.5)}$	1.48703E-06	7.25975E-09	2.61713E-07	5.26747E-06	5.71902E-06	4.35177E-06	1.71131E-06	1.88056E-05
OC	8.64813E-07	4.49864E-09	1.56781E-07	3.37389E-06	3.46992E-06	2.41574E-06	9.04414E-07	1.11901E-05
BC	5.06166E-07	2.55391E-09	8.79298E-08	1.84864E-06	1.90694E-06	1.4237E-06	5.62018E-07	6.33794E-06
TPM	1.15916E-06	5.42729E-09	2.5641E-07	4.67646E-06	5.46838E-06	4.0042E-06	1.26085E-06	1.68309E-05
NMHC	1.30527E-06	7.36347E-09	2.08991E-07	5.18778E-06	4.78895E-06	3.06703E-06	1.27521E-06	1.58406E-05

Figure 1. IRS-P6 AWiFS classified image of Northeast India.

tion of Northeast India, which typically occurs at an altitude of 900 m asl, faces severe threat due to shifting cultivation. The evergreen rainforests found in Assam valley, lower parts of the Himalayas and Naga Hills have been extensively fragmented due to shifting cultivation. Around 0.45 million families in the northeastern region cultivate 10,000 sq. km of forests. With the increase in population, the jhum cycle has decreased to 5 years from 20 to 30 years in the past.

Multi-temporal datasets of AWiFS from January to May 2005 were considered for the present study. AWiFS is a wide-angle medium resolution (56 m) camera with a swath of 740 km (FOV = ± 25°), on-board RESOURCESAT-1 remote sensing satellite, built by Indian Space Research Organization (ISRO). The push-broom instrument operates in four spectral bands. The AWiFS camera is realized using two separate opto-electronic modules that are tilted by 11.94° with respect to the nadir. Each module covers a swath of 370 km, providing a combined swath of 740 km with a side lap between them. The wide swath coverage enables AWiFS to provide a five-day repeat capability. The optoelectronic modules contain refractive imaging optics along with band-pass interference filter, a neutral density filter and a 6000 pixel linear array CCD detector for each spectral band.

Daily DMSP–OLS night-time satellite data from January to May 2005 were processed for active fires over the north-eastern region. DMSP operates F15 and F16 satellites in sun-synchronous orbits with night-time overpasses ranging from about 7 to 10 pm local time. The OLS is an oscillating scan radiometer with two spectral bands; visible and near-infrared portion (0.5 to 0.9 μm) of the spectrum, and the thermal bandpass covers the 10.5 to 12.5 μm region. At night, the visible band is intensified with a photo-multiplier tube to permit detection of clouds illuminated by moonlight. Light intensification enables observation of faint sources of visible–near infrared emissions present at night on the earth's surface, including cities, towns, villages, gas flares, heavily-lit fishing boats and fires[20]. Basic procedures adapted in deriving DMSP–OLS fires are given by Elvidge *et al.*[21]. Derived night-time fire images were compiled into 15-day composites and compared with state-wise emissions to understand the cause–effect relationships.

The multi-temporal AWiFS datasets were geo-referenced to a base map within an error of one pixel (sub-pixel accuracy) and brought to one common projection. Digital number values were converted to top of the atmospheric (TOA) reflectance and TOA corrected datasets were subjected to maximum likelihood classification using hybrid approach. Misclassified areas were carefully identified and re-classified through interactive editing to improve accuracy. Accuracy assessment has been done on classified images by

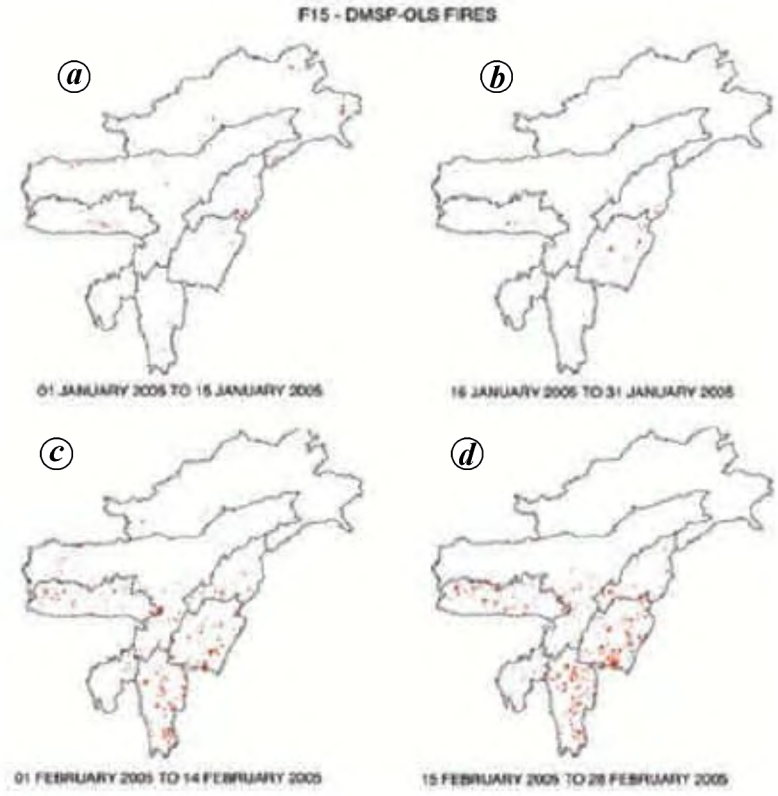

Figure 2 *a–d.* Fortnightly composites of DMSP–OLS-derived fire locations during January–February 2005.

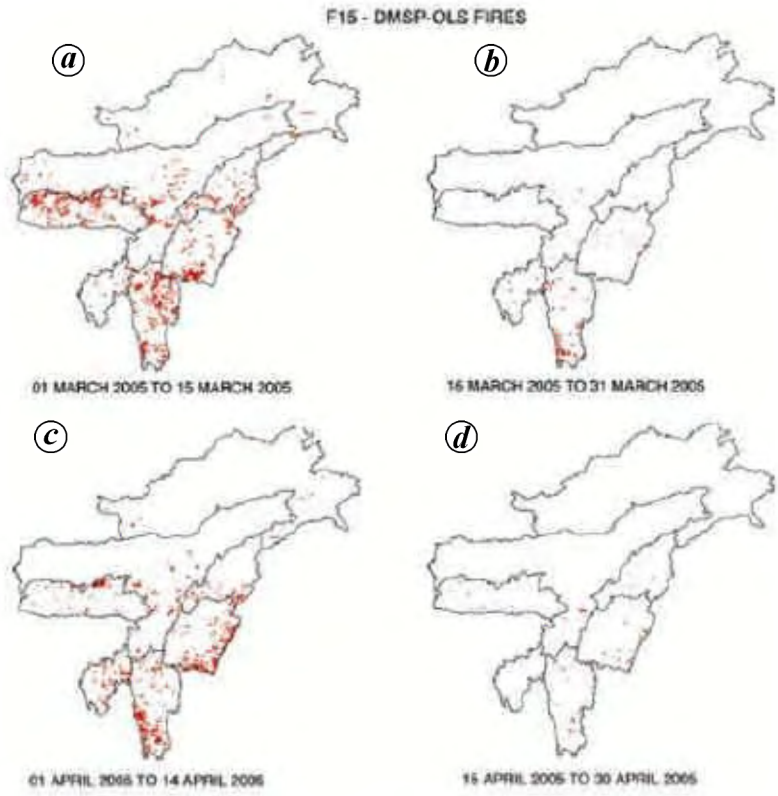

Figure 3 *a–d.* Fortnightly composites of DMSP–OLS-derived fire locations during March–April 2005.

deriving confusion matrices and kappa coefficient for individual images. State-wise area statistics of different vegetation types as well as burnt areas in each vegetation type has been derived from the classified outputs.

Ground measurements done for a few sites on pre-fire, during-fire and post-fire emissions of trace gases were used to derive the local emission factors (EF) for different gas species like CO_2, CO, CH_4, N_2O, NO_x and NMHCs. Emission factors for the rest of the sites were taken from the literature to quantify the emissions[16]. Acreage burnt was taken from the classified images for each state in order to quantify the emissions.

Emissions from burnt areas were estimated by applying the following expression: Emissions (g) = Emission factor (g/ton) × fuel consumption (tons/ha) × area burned (ha).

Fuel combustion efficiency was taken as 40%, and for bamboo it was considered as 100%.

Figure 1 shows a mosaic of state-wise classified map of the study area derived from IRS-P6 AWiFS data. The study area comprises predominantly tropical evergreen, semi evergreen, temperate and mixed moist deciduous forests, which are subjected to annual fires. Spatial pattern of burnt areas from Figure 1 clearly suggests that shifting cultivation is widespread over all the states in the northeast and in all forest types. Classified images of the study area clearly discriminated the burnt areas and burnt area statistics derived from the AWiFS datasets suggested the highest burnt area in Mizoram (736 sq. km) followed by Nagaland (547 sq. km), and Meghalaya. Emission factors were taken as EF-CO_2, 1.58 g/kg; EF-CO, 0.104 g/kg; EF-CH_4, 0.0068 g/kg; EF-NO, 0.0016 g/kg; EF-N_2O, 0.002 g/kg; EF-$PM_{2.5}$, 0.0091 g/kg; EF-OC, 0.0052 g/kg; EF-BC, 0.00066 g/kg; EF-TPM, 0.0065 g/kg; EF-NMHC, 0.0081 g/kg. Calculated total emissions suggested 3.5×10^{-3} Tg of CO_2, 2.0×10^{-4} Tg of CO, 1.32×10^{-5} Tg of CH_4, 5.9×10^{-6} Tg of NO, 4.95×10^{-7} Tg of N_2O, 1.88×10^{-5} Tg of $PM_{2.5}$, 1.19×10^{-5} Tg of OC, 6.33×10^{-6} Tg of BC, 1.6×10^{-5} Tg of TPM and 1.58×10^{-5} Tg of NMHC from shifting cultivation areas. Table 1 shows state-wise statistics of total emissions. These trace gases have several atmospheric and ecological implications. As shifting cultivation is practised over large areas in the Indian region, it forms a primary source of greenhouse gases.

Availability of land for agriculture in the northeastern region (21%) is limited due to geophysical parameters compared to other regions of India (54%), which puts pressure on the forests. The economics and efficiency of jhum cultivation[22] showed that jhum is a resourceful system of organic multiple cropping well suited to heavy-rainfall areas. The economic and energetic efficiency of jhum is higher than alternative forms of agriculture, such as terrace and valley cultivation with respect to expensive inputs such as fertilizers, and is thus followed by the tribals.

Figures 2 *a–d* and 3 *a–d* show 15-day composite images of DMSP–OLS-derived night-time fires over the study area from January to April 2005. DMSP–OLS analysis suggests enhanced fire activity during the first and second week of March in all the States. Mizoram, Nagaland, Meghalaya and Manipur showed fires during all the four months, with a peak in March and April.

1. Gubbi, S., *Deccan Herald*, Bangalore, available at http://wildlifefirst.info/images/wordfiles/fire.doc (accessed January 2004), 2003.
2. Stracey, P. D., *J. Bombay Nat. Hist. Soc.*, 1967, **64**, 440–446.
3. Hao, W. M., Ward, D. W., Olbu, G. and Baker, S. P., *J. Geophys. Res.*, 1996, **101**, 23577–23584.
4. Fearnside, P. M., *Climate Change*, 2000, **46**, 115–158.
5. Crutzen, P. J. and Andreae, M. O., *Science*, 1990, **250**, 1669–1678.
6. Dwyer, E., Gregoire, J. M. and Malingreau, J. P., *Ambio*, 1998, **27**, 175–181.
7. Hao, W. M. and Liu, M. H., *Global Biogeochem. Cycles*, 1994, **8**, 495–503.
8. Kaufman, Y. J. *et al.*, *J. Geophys. Res.*, 1998, **103**, 32215–32238.
9. Christopher, S. A., Chou, J., Zhang, J., Li, X. and Welch, R. M., *Geophys. Res. Lett.*, 2000, **27**, 2197–2200.
10. Reid, J. S. *et al.*, *Atmos. Chem. Phys.*, 2005, **5**, 827–849.
11. Kaufman, Y. J. *et al.*, *J. Geophys. Res.*, 1998, **103**, 31783–31808.
12. Levine, J. S., Cofer III, W. R., Cahoon, D. R. and Winstead, E. L., *Environ. Sci. Technol.*, 1995, **29**, 120A–125A.
13. Cofer III, W. R. *et al.*, *J. Geophys. Res. D*, 1989, **94**, 2255–2259.
14. Hurst, D. F., Griffith, D. W. T. and Cook, G. D., *J. Geophys. Res.*, 1994, **99**, 16441–16456.
15. Yokelson, R. J., Susott, R., Ward, D. E., Reardon, J. and Griffith, D. W. T., *J. Geophys. Res.*, 1997, **102**, 18865–18877.
16. Andrae, M. O. *et al.*, Trace gas and aerosol emissions from Savanna fires. In *Biomass Burning and Global Change, Remote Sensing, Modeling and Inventory Development and Biomass Burning* (ed. Levine, J. S.), MIT Press, 1996, pp. 278–295.
17. Ahern, F., Gregoire, J.-M. and Justice, C., Report of a workshop, Joint Research Center, ISPRS, Italy, 3–5 November 1999.
18. Korontzi, S., Justice, C. O. and Scholes, R., *J. Arid Environ.*, 2003, **54**, 395–404.
19. Champion, H. G. and Seth, S. K., *Revised Survey of the Forest Types of India*, Government of India, Delhi, 1968.
20. Elvidge, C. D., Baugh, K. E., Kihn, E. A., Kroehl, H. W. and Davis, E. R., *Photogramm. Eng. Remote Sensing*, 1997, **63**, 727–734.
21. Elvidge, C. D., Nelson, I., Hobson, V. R., Safran, J. and Baugh, K. E., Detection of fires at right using DMSP–OLS Data. *Global and Regional Fire Monitoring from Space*, MIT Press, 2001, pp. 125–144.
22. Ramakrishnan, P. S., *Shifting Agriculture and Sustainable Development: An Interdisciplinary Study from North–Eastern India*, MAB Series, UNESCO, Paris, 1992, vol. 10.

ACKNOWLEDGEMENTS. We are grateful to the Director and Dy. Director (RS&GIS-AA), NRSA, Hyderabad for encouragement, and ISRO–GBP for funding.

Received 25 July 2006; revised accepted 16 November 2006

T. R. KIRAN CHAND
K. V. S. BADARINATH*

Forestry and Ecology Division,
National Remote Sensing Agency
(Department of Space, Govt of India),
Balanagar,
Hyderabad 500 037, India
**For correspondence*
e-mail: badrinath_kvs@nrsa.gov.in

Mutational analysis of H5N1 and H1H1 for ascertaining test systems

Bird flu (also known as avian influenza, avian flu, influenza virus A, type A flu, or genus A flu) is a type of influenza virus that is hosted by birds, but may infect several species of mammals. H5N1 is a highly pathogenic strain of bird flu. The first known appearance of this type of influenza in humans[1] was in Hong Kong during 1997. The name H5N1 refers to the subtypes of surface antigens present on the virus: hemagglutinin type 5 and neuraminidase type 1. Normally, avian flu viruses are transported worldwide in the intestines of wild birds, and are non-lethal. Infected birds pass on H5N1 through their saliva, nasal secretions and faeces. Because migratory birds are among the carriers of the H5N1 virus, it may spread to all parts of the world. There are three types of influenza viruses, namely A, B and C, which are classified on the basis of nucleoproteins. Among these, influenza A virus has a pandemic potential. There are two important surface glycoproteins, hemagglutinin (HA), and neuraminidase (NA), which are embedded in the virus membrane. Hemagglutinin mediates receptor binding and membrane fusion, whereas neuraminidase facilitates cleavage of the viral progeny from infected cells. There are 16 H and 9 N subtypes of the influenza A virus[2]. Totally 144 HA and NA combinations are possible, out of which 103 have been confirmed. The avian influenza A virus (AIV) that contains the HA subtypes H3, H4, H6 is the most frequently isolated, whereas AIV of subtypes H5 and H7 was less frequently encountered. All other HAs are rather rare. AIV that possesses the NA of subtypes N2, N1, N8 and N3 is frequent and all other NAs are rarely detected[3].

Figure 1. Protein structure of *PB2* gene of H5N1 genome which has a mutation at position 627.